Met. Mater. Int., Vol. 23, No. 4 (2017), pp. 798~804
doi: 10.1007/s12540-017-6714-9

Effect of the Cr_2O_3 and TiO_2 as Nucleating Agents in SiO_2-Al_2O_3-CaO-MgO Glass-Ceramic System

Gu-Seul Back[1], Mi-Jung Yoon[2], and Woo-Gwang Jung[1,*]

[1]Department of Advanced Materials Engineering, Graduate School of Kookmin University, Seoul 02707, Republic of Korea
[2]Dongdo Basalt Industry Co. Ltd., Gyeongju 38028, Republic of Korea

(received date: 8 October 2016 / accepted date: 29 November 2016)

The nucleation agent is one of the most important factors in glass-ceramics as it can control either the crystallization temperature or the activation energy. In this study, we investigated the effect of two common nucleation agents, TiO_2 and Cr_2O_3, in the SiO_2-Al_2O_3-CaO-MgO system. To determine the effect of TiO_2 and Cr_2O_3 on nucleation, we measured the crystallization temperature by differential scanning calorimetry (DSC) scanning. To determine the activation energy of nucleation, the DSC scanning was made for the selected samples at various speeds. Also, the crystallinity of the selected sample was evaluated from the scattering intensity in X-ray diffractometry. Using DSC scanning, we found that TiO_2 was effective in decreasing the crystallization temperature, while Cr_2O_3 was effective in decreasing the activation energy. We also performed nucleation heat treatment near the glass transition point. It is found that nucleation heat treatment was not effective in decreasing the crystallization temperature in our experimental condition. The XRD scattering method results showed that temperature is the key factor in crystallization and the effect of time is not as important.

Keywords: glass-ceramics, crystallization, recycling, nucleation agent, Kissinger method

1. INTRODUCTION

Glass-ceramics are defined as materials produced under controlled heat to crystallize the base glass. Glass-ceramics have the outstanding characteristics of both glass and crystallite: the moisture resistance and easy formation of glass, and the high mechanical strength and chemical resistance of crystallite. Hence, glass-ceramics have been widely used in civil engineering, chemical engineering, electrical engineering, and the space industry.

A wide variety of compositions are available in glass-ceramics, with very different properties, depending on the composition system [1-5]. Beginning in the early 1960s, glass ceramic materials have been actively developed for recycling industrial wastes such as metallurgical slags, which offered the significant potential for cost saving. Glass-ceramics have also been widely studied with respect to the use of various metallurgical wastes including blast furnace slag [6-8], aluminum residue [9], phosphorus slag [10], copper slag [11], nickel slag [12], and steel slag [13]. Recently, we also investigated the possibility using steel industry slags and some industrial wastes to prepare glass ceramic materials characterized by high strength and high anti-abrasion properties [14].

In glass-ceramics, crystallinity is one of the most important factors. Field [15] studied the crystallinity of stretched rubber using X-ray diffractometry to measure scattering intensity, and demonstrated that scattering intensity decreases proportionally as the material is crystallized. Based on Field's experiment, Ohlberg and Strickler [16] applied this theory to glass-ceramics to determine degrees of crystallization. Jang and Jung [17] also applied this theory to glass-ceramics in a CaO-MgO-Al_2O_3-SiO_2(-Na_2O) system, and further deduced the Avrami factor. Karamanov and Pelino [18] determined the degree of crystallization in glass-ceramics by measuring density.

To facilitate glass crystallization, a nucleation agent can be added in the manufacture of glass-ceramics. Commonly used nucleation agents include Cr_2O_3, Fe_2O_3, TiO_2, ZrO_2, P_2O_5, and some halide minerals such as CaF_2. Baldi and Generali [19] have used TiO_2, ZrO_2, and P_2O_5 as nucleation agents in SiO_2-CaO-MgO systems, Banijamail *et al.* [20] used TiO_2, CaF_2, and ZrO_2 in SiO_2-Al_2O_3-CaO systems, and Alizadeh and Marghussian [21] used WO_2, V_2O_5, and MoO_2 in SiO_2-CaO-MgO-Na_2O systems. Karamanov *et al.* [22] used small amounts of Cr_2O_3 in SiO_2-Al_2O_3-CaO-Na_2O with a higher amount of Fe_2O_3. As is evident, there is a diverse range of nucleation agents and their behavior is complicated, based on the system composition.

*Corresponding author: wgjung@kookmin.ac.kr

In our present work, we investigated the effect of Cr_2O_3 and TiO_2 on the crystallizing behavior of the SiO_2-Al_2O_3-CaO-MgO glass-ceramic system with specific amounts of Fe_2O_3, which is a common composition system in basalt material. In the SiO_2-Al_2O_3-CaO-MgO system, we found the main phases to be augite and anorthite, which have been reported previously [23,24]. We used various experimental facilities to quantitatively evaluate the effects of Cr_2O_3 and TiO_2 as nucleating agents in this system.

2. EXPERIMENTAL PROCEDURE

2.1. Preparation of glass sample

We designed the glass composition to include SiO_2, MgO, CaO, and Al_2O_3, and added Fe_2O_3 and MnO to reduce viscosity and make the casting process easier. To examine the effect of nucleating agents, we added Cr_2O_3 and TiO_2 and adjusted other glass components in proportion to the amount of the added nucleating agent. Tables 1 and 2 show the specific composition of the samples used in our Cr_2O_3 and TiO_2 experiments, respectively. We prepared CaO by calcinating $Ca(OH)_2$ at 900 °C, and used reagent-grade chemicals as starting materials. We mixed the weighed materials in a mortar first, then treated the mixed powder with a ball mill, using silicon balls, at 200 rpm for 20 min.

Next, we put the mixture into an alumina crucible and placed the crucible in an electrical-resistance furnace. We set the furnace to slowly raise temperature to 1500 °C, and to ensure that the mixture was melted and completely mixed in the crucible, we kept the temperature constant at 1500 °C for one hour. While the furnace temperature was increasing to 1500 °C, we set another furnace to increase its temperature to 500 °C to pre-heat a graphite mold for 10 min, just prior to casting. After an hour at 1500 °C, we casted the melt in the pre-heated mold. After casting, we put both the mold and casted glass into the pre-heated furnace at 500 °C to prevent the glass from breaking, and slowly cooled the mold and glass sample in the furnace.

2.2. Characterization

The chemical composition of the materials was determined by X-ray fluorescence (XRF) and the result of composition analysis is shown in Tables 1 and 2. Figure 1 shows the composition of samples in SiO_2-Al_2O_3-CaO with 16 wt% of MgO. It is noteworthy that all samples are in the range of liquid region

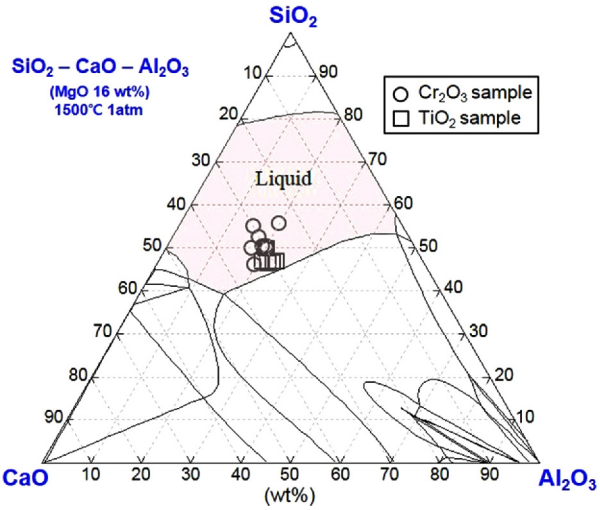

Fig. 1. Composition of glass samples on phase diagram of SiO_2-Al_2O_3-CaO with MgO 16 wt% at 1500 °C.

Table 1. Composition of glass ceramics for Cr_2O_3 nucleation experiment (wt%)

Sample	SiO_2	Al_2O_3	MnO	CaO	MgO	Fe_2O_3	Cr_2O_3
CR0.00	42.82	17.26	7.20	12.51	13.17	4.48	-
CR0.11	39.56	17.05	7.15	13.88	12.67	4.52	0.11
CR0.15	40.40	16.66	7.06	13.94	13.20	4.78	0.15
CR0.38	42.13	16.87	7.10	13.91	12.40	4.54	0.38
CR0.57	42.01	16.98	7.22	12.41	13.18	4.68	0.57
CR0.84	47.02	17.58	6.70	10.99	11.29	4.17	0.84
CR3.35	39.61	16.50	7.10	10.89	12.42	5.00	3.35
CR3.57	40.51	14.28	6.76	13.21	12.07	5.05	3.57
CR9.44	40.17	12.05	7.51	10.34	11.67	5.05	9.44
CR14.9	35.02	11.73	7.67	10.23	10.41	5.50	14.99

Table 2. Composition of glass ceramics for TiO_2 nucleation experiment (wt%)

Sample	SiO_2	Al_2O_3	MnO	CaO	MgO	Fe_2O_3	TiO_2
TI0.00	42.82	17.26	7.20	12.51	13.17	4.48	-
TI4.04	39.70	18.65	7.05	12.61	12.22	4.42	4.04
TI7.63	37.72	19.20	7.10	11.73	11.42	4.16	7.63
TI8.50	37.49	20.54	6.95	10.80	10.69	4.02	8.50
TI9.34	37.39	20.37	6.83	10.90	10.38	3.86	9.34

in the diagram. After the cool-down period, to measure the material's properties, we crushed each glass sample into powder and conducted differential scanning calorimetry (DSC) on a Mettler Toledo TGA/DSC1 instrument. We did not perform thermogravimetric analysis, as the change in the glass sample weight by temperature was negligible. We conducted DSC analysis in a temperature range of 600 °C to 1500 °C at a heating rate of 10 °C/min, and purged Ar gas during the analysis. For the DSC measurement, we used a high-purity alumina pan of 70 ml with a cover.

We then carried out X-ray diffraction (XRD) analyses on a Rigaku D/max 2500 (Rigaku Japan) under a voltage of 40 kV and a current 200 mA by Cu Kα radiation on the cold pressed powders of glass or ceramic. We used the amorphous scattering method to measure the degree of crystallization, since most of the samples were in powder form, making it difficult to measure the density.

2.3. Nucleation and Growth procedures

From our DSC analyses, we determined the glass transition points. We then provided some part of samples of selected composition for heat treatment (the nucleation test) near to their glass transition points. Here we used two furnaces in the nucleation heat treatment. We put the samples into a small alumina crucible, and kept them at the desired temperature for 1 h in main furnace. After 1 h of nucleation, we moved the sample and crucible into the other furnace, which we set at 500 °C for 10 min. Finally, we took the crucible out from the 500 °C furnace and covered it with Kaowool insulation to cool slowly. Then, we again performed DSC measurement on the samples with nucleation treatment to examine the effect of this procedure on their crystallization behavior, which has also been studied by Karamanov *et al.* [22].

We performed the crystal growth treatment with different time on selected samples, each time performing the similar procedure as the nucleation heat treatment. We put the samples into alumina crucibles and treated them at the desired crystallization temperature, as determined by DSC analysis. After treating the samples for a specified time, we moved them into the other furnace, which was set at 500 °C, and kept them there for 10 min before taking them out of the furnace and covering them with Kaowool insulation for slow cooling.

In this study, we varied the crystallization time to examine the effect of time on the crystallization of the glass-ceramic material. After crystallization, we analyzed the samples by XRD to evaluate their crystallinity. To do this, we first scanned the samples from 20 to 80 degrees, and then measured the scattering intensity near the highest main peak. We made a precise measurement in the range from 28.7 to 28.8 degrees, with a step of 0.02. At each point, we measured the intensity for 200 s, and then used the average intensity to evaluate the crystallinity.

3. RESULTS AND DISCUSSION

3.1. Cr_2O_3 as nucleating agent and nucleation process

Figure 2 shows the DSC data of the Cr_2O_3-containing glass. In a wide range of Cr_2O_3 concentrations from CR0.11 to CR14.9, the temperature of the crystallization peak was higher than 0 wt% Cr_2O_3. Between CR0.15 and CR0.38, the crystallization peak temperature decreased slightly, but was still higher than the temperature without Cr_2O_3. Figure 3 shows the equilibrium phases for the CR3.35 composition, as calculated by FactSage software. The composition that includes Cr_2O_3 formed the spinel phase $MgCr_2O_4$ even at 1500 °C. We expected that the spinel phase boundaries could act as nucleation sites, to make the crystallization much easier, and that the crystallization temperature would decrease. Decreasing crystallization temperature by the spinel phase has been reported by other researchers [25-28]. In contrast, several studies have also reported that Cr_2O_3 increased the crystallization temperature [29,30]. In this study, we evaluated the effect of Cr_2O_3 as a nucleating agent not only with respect to changes in the crys-

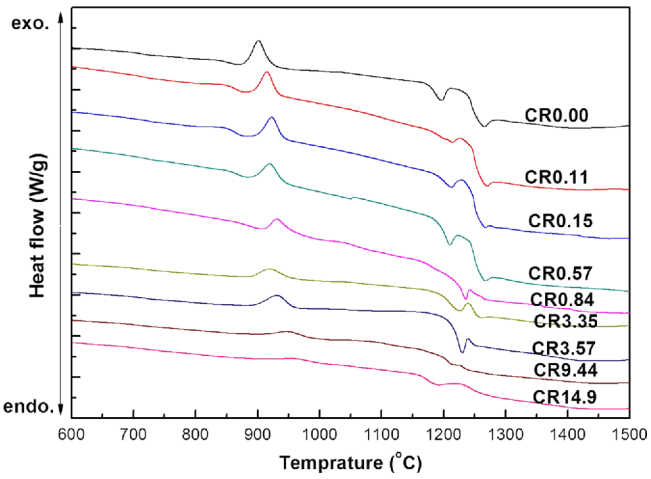

Fig. 2. DSC profiles of Cr_2O_3 nucleating experiment.

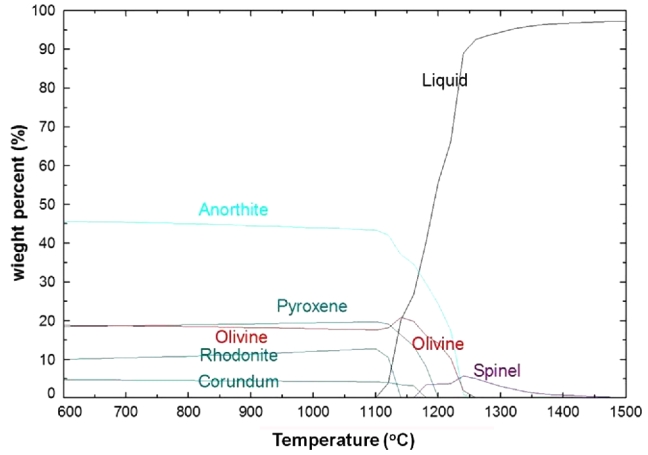

Fig. 3. Equilibrium phases in terms of temperature calculated by FactSage for CR3.35 composition.

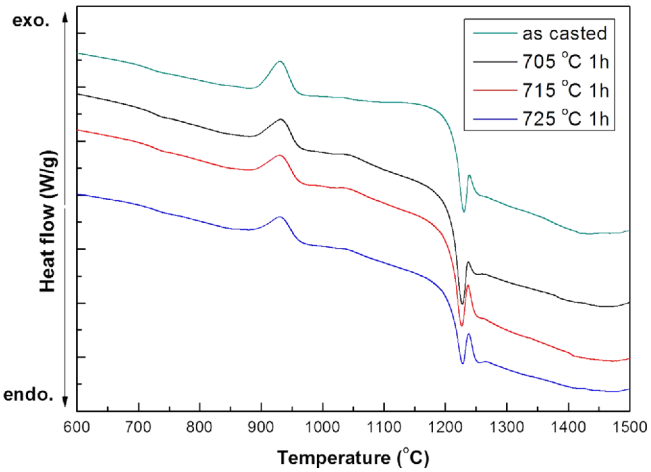

Fig. 4. DSC scan of CR3.57 composition with nucleation heat treatment.

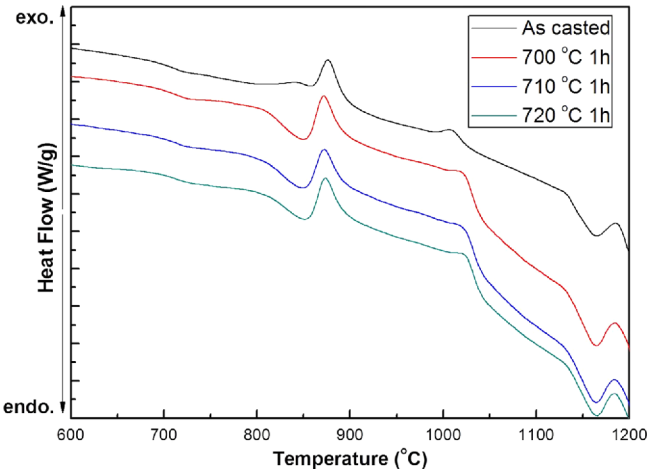

Fig. 6. DSC scan of TI8.50 composition with nucleation heat treatment.

tallization temperature, but also in the activation energy, calculated using the Kissinger equation [31].

Figure 4 shows the DSC profiles for CR3.57 after the nucleation process for different temperatures. The differences in the crystallization temperature are less than 5 °C, so the nucleation process has almost no effect on decreasing the crystallization temperature.

3.2. TiO_2 as nucleating agent and nucleation process

Figure 5 shows the DSC data of TiO_2-containing glass. The crystallization temperature decreased as the TiO_2 weight percent increased. In particular, between TI7.63 and TI8.50, the change in the crystallization temperature was 15 °C, while other changes were 5-6 °C. This data indicates that TiO_2 helps to decrease crystallization temperature in this composition. Using TiO_2 to decrease the crystallization temperature has been reported by other researchers [32-34]. As the TI8.50 shows a rapid decrease in crystallization temperature, we conducted the following experiment with this composition.

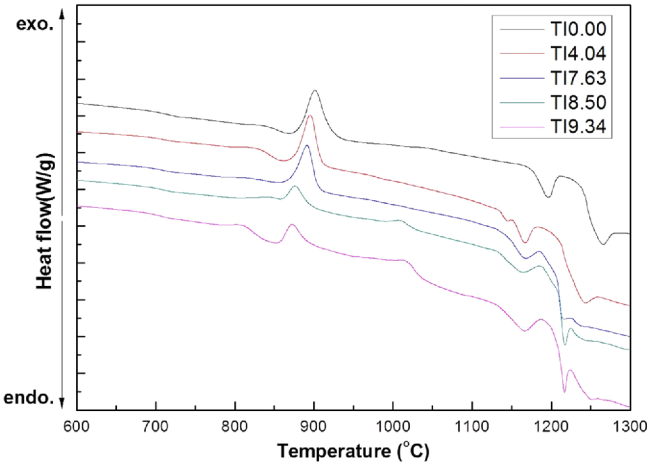

Fig. 5. DSC scan of TiO_2 added samples.

We performed the nucleation process with the TI8.50 composition. According to the DSC data, the nucleation temperature is near to the glass transition point, which is 705 °C. We carried out the nucleation process by putting the sample into the furnace, which we set at 705 °C, 710 °C, 715 °C, and 720 °C, in turn. Figure 6 shows the DSC data results after nucleation. Similar to that for the Cr_2O_3-added samples, the crystallization temperature decreased slightly after nucleation, negligibly so. The differences only ranged 1-2 °C, while another study reported this temperature to have reduced by as much as 20 °C or more [22]. Our study results show that the nucleation process of the SiO_2-Al_2O_3-CaO-MgO system with TiO_2 is not effective in decreasing the crystallization temperature.

3.3. Activation Energy by Kissinger method

To obtain the activation energy of the sample, we used the Kissinger method. We selected glass samples without any nucleating agent for the CR0.84 and TI8.50 samples and conducted DSC analysis at different heating rates of 5 °C/min, 10 °C/min, 15 °C/min, 20 °C/min, and 30 °C/min. The crystallization temperature changed with changes in the heating rate. Table 3 lists the crystallization temperatures and Fig. 7 shows the DSC data for different heating rates. Figure 8 shows the data plotted using the Kissinger equation, which

Table 3. The list of peak temperature of each samples with different DSC scan speed

T_p (°C)	5 °C/min	10 °C/min	15 °C/min	20 °C/min	30 °C/min
Non-nucleted-glass	883	901	912	920	931
CR0.84	896	919	932	944	960
TI8.50	857	876	886	891	905

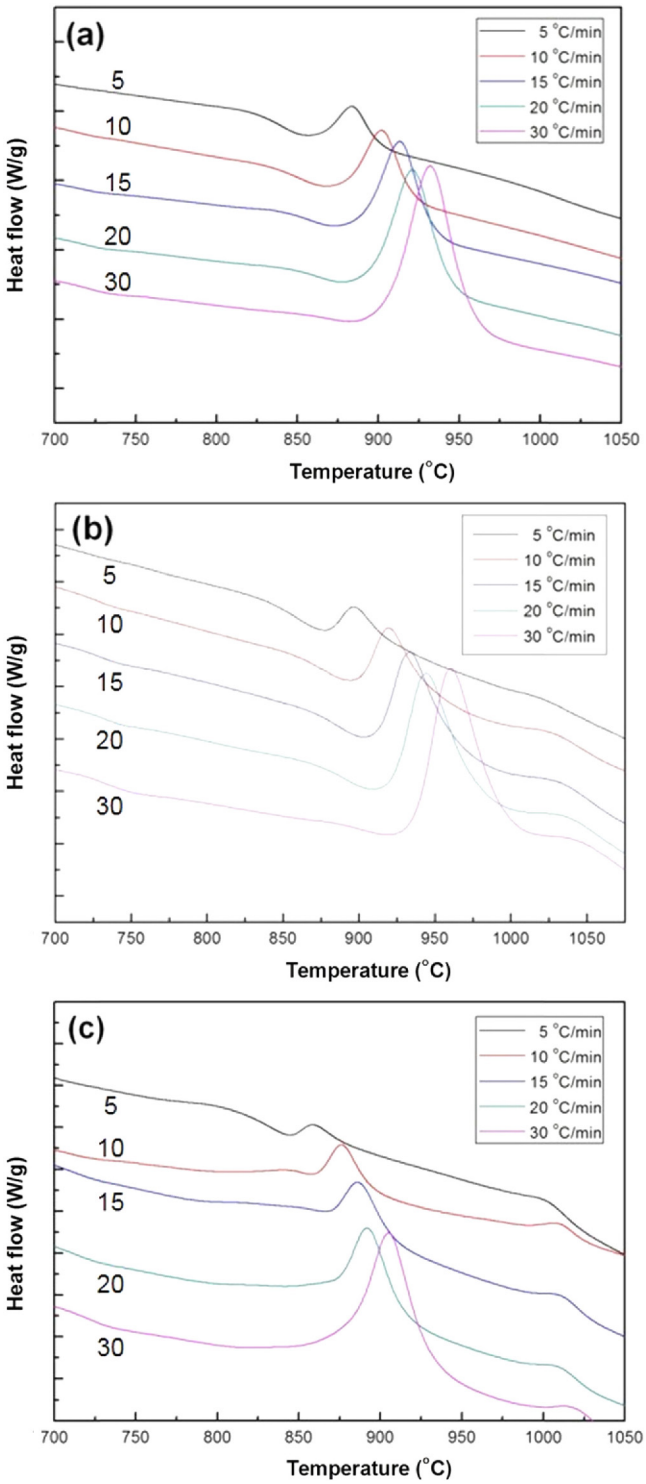

Fig. 7. DSC scan with different scan speeds: (a) non-nucleated glass, (b) CR0.84, and (c) TI8.50.

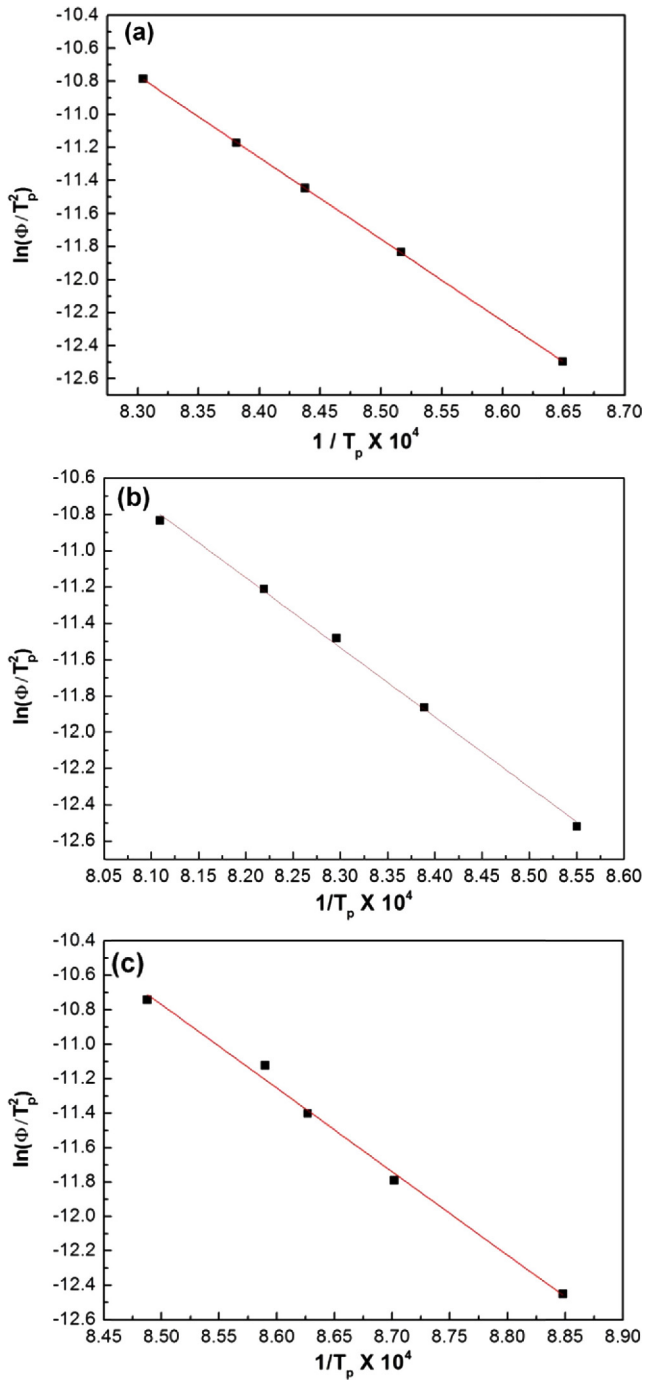

Fig. 8. The linear fitting based on the Kissinger equation: (a) non-nucleated glass (b) CR0.84 (c) TI8.50.

is given as

$$\ln\left(\frac{\phi}{T_p^2}\right) = \frac{-E_c}{RT_p} + \text{constant} \quad (1)$$

where ϕ is the DSC heating rate, E_c is the heating rate, R is the gas constant, and T_p is the crystallization temperature. In Fig. 8, we adopted a linear fitting, and found the activation energy to be 411.44 kJ/mol for the non-nucleating-agent sample, 319.59 kJ/mol for the CR0.84 sample, and 403.13 kJ/mol for the TI8.50 sample. As such, the samples with a nucleating agent showed a lower activation energy, and the CR0.84 sample, in particular, showed a much lower energy than the TI8.50

Table 4. The list of activation energy reported by other researchers

Author	Composition System	Phases	E_c (kJ/mol)
P. Alizadeh, V.K. Marghussian [35]	SiO_2, MgO, CaO, Na_2O, Fe_2O_3,Cr_2O_3	Wollastonite, Diopside, cristobalite	693.2
Y.J. Park, J. Heo [36]	SiO_2, CaO, MgO, Al_2O_3, TiO_2, Na_2O	Diopside	499
M.L Overcoglu, B. Kuban & H. Ozer [37]	SiO_2, CaO, MgO, Al_2O_3, TiO_2, Alkali oxide	Diopside, TiO_2	150
M. Romero, R. D. Rawlings and J. Ma. Rincon [38]	SiO_2, Al_2O_3, TiO_2, Li_2O, MgO,	b-spodumene	282.4

Table 5. Amorphous scattering intensity of TI8.50 sample

	As casted	30 min	60 min	120 min	240 min
876 °C	103,635	57,979	52,229	42,432	40,613
900 °C	103,635	23,637	23,591	21,857	19,095

sample, although the crystallization temperature had not been decreased. Table 4 shows the activation energies reported for other compositions. We note that the activation energies are diverse with respect to the system and composition.

3.4. Crystallinity

To measure crystallinity, we used X-ray diffraction scattering method. We crystallized the samples at 876 °C and 900 °C for 30 min, 60 min, 120 min, and 240 min, respectively. By assuming that a 240-min heat-treated sample at 900 °C is completely crystallized and the mother glass sample is completely amorphous, we calculated the crystallinity using the following equation:

$$\text{Crystallinity (\%)} = \frac{I_g - I_x}{I_g - I_c} \times 100 \quad (2)$$

where I_g is the intensity of glass, I_x is the intensity of the sample, and I_c is the intensity of crystallites.

The measurement of degree of crystallization was made for TiO_2 8.50 wt% sample. Table 5 shows the results of this experiment, and Fig. 9 shows the crystallinity with respect to time. The lowest amorphous value occurred in the 900 °C, 240-min heat-treated sample, so we set it as having been 100% crystallized, the I_c. 900 °C heat-treated samples show lower intensity than the 876 °C heat-treated samples, even though the treatment time is much longer. At both temperatures, the differences between 120 min and 240 min is not large. Based on these data, we can conclude that temperature is the primary factor in the crystallization, while the time is only a minor factor in our experimental condition.

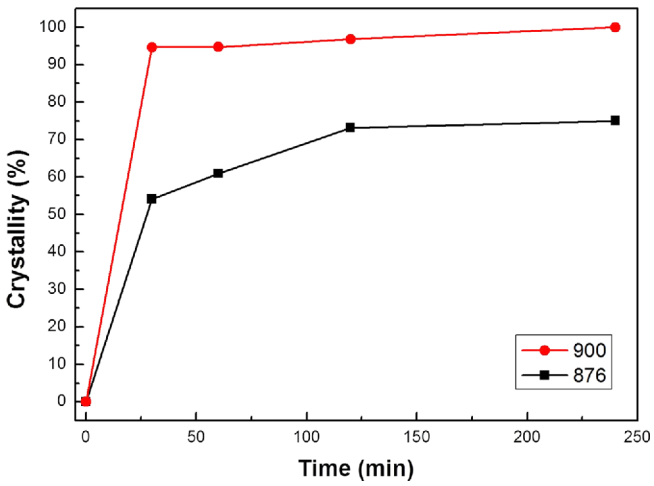

Fig. 9. Change in degree of crystallization with different heat treatment time and temperature for TI8.50.

4. CONCLUSION

We added Cr_2O_3, and TiO_2 to the SiO_2-Al_2O_3-CaO-MgO system as nucleating agents, and evaluated the effect on nucleation and crystallization by DSC and amorphous scattering measurement. We found addition of Cr_2O_3 to increase the crystallization temperature, while addition of TiO_2 decreased it. In particular, there was a bigger difference in crystallization temperature between the TI8.50 and TI7.63 samples than between other compositions. We have made nucleation heat treatment near the glass transition temperature to check the effect of nucleation heat treatment. However, the effect was not recognized for the samples with Cr_2O_3 or TiO_2 added samples. The activation energy were measured for the non-nucleated-glass, CR0.84, and TI8.50 samples by the Kissinger method. The activation energies were measured to be 411.44 kJ/mol, 319.59 kJ/mol, and 403.13 kJ/mol in the non-nucleated glass, CR0.84, and TI8.50 samples, respectively. It is found that Cr_2O_3 addition may decrease the activation energy of crystallization. We measured the degree of crystallization by the amorphous scattering method for different times and temperatures. At a high temperature, the glass-ceramic shows high crystallinity despite the shorter heat treatment time than at the lower temperature, which means that temperature is the key factor determining the degree of crystallization.

ACKNOWLEDGEMENT

This study was supported by the Korea Institute of Energy Technology Evaluation and Planning (KETEP) and funded by the Ministry of Trade, Industry and Energy (No.: 20145010600040).

REFERENCES

1. R. N. McNally and G. H. Beall, *J. Mater. Sci.* **14**, 2596 (1979).
2. T. Kokubo, S. Ito, and S. Sakka, *J. Mater. Sci.* **21**, 536 (1986).
3. J. Tamura, K. Kawanabe, M. Kobayashi, T. Nakamura, T. Kokubo, S. Yoshihara, *et al. J. Biomed. Mater. Res. A* **30**, 85 (1996).
4. O. P. Thakur, D. Kurmar, O. Parkash, and L. Pandey, *Mater. Lett.* **23**, 253 (1995).
5. W. Y. Zhang, H. Hao, and Y. Xu, *J. Eur. Ceram. Soc.* **31**, 1669 (2011).
6. A. A. Francis, *J. Euro. Ceram. Soc.* **24**, 2819 (2004).
7. S. M. Salman and H. Darwish, *Ceramics* **50**, 88 (2006).
8. H. Liu, H. Lu, D. Chen, H. Wang, H. Xu, and R. Zhang, *Ceram. Int.* **35**, 3181 (2009).
9. A. Lopez-Delgado and H. Tayibi, *Waste Manage. Res.* **30**, 474 (2012).
10. J. W. Cao and Z. Wang, *J. Alloy. Compd.* **557**, 190 (2013).
11. Z. Yang, Q. Lin, J. Xia, Y. He, G. Liao, and Y. Ke, *J. Alloy. Compd.* **574**, 354 (2013).
12. Z. J. Wang, W. Ni, Y. Jia, L. P. Zhu, and X. Y. Huang, *J. Non-Cryst. Solids* **356**, 1554 (2010).
13. F. He, Y. Fang, and J. Xie, *Mater. Design* **42**, 198 (2012).
14. G. S. Back, H. S. Park, S. M. Seo, and W.-G. Jung, *Met. Mater. Int.* **21**, 1061 (2015).
15. J. E. Field, *J. Appl. Phys.* **12**, 23 (1941).
16. S. M. Ohlberg and D. W. Strickler, *J. Am. Ceram. Soc.* **45**, 170 (1962).
17. S. H. Jang and H. J. Jung, *J. Korean Ceram. Soc.* **17**, 20 (1980).
18. A. Karamanov and M. Pelino, *J. Eur. Ceram. Soc.* **19**, 649 (1999).
19. G. Baldi and E. Generali, *J. Mater. Sci.* **30**, 3251 (1995).
20. S. Banijamali, B. E. Yekta, H. R. Rezaie, and V. K. Marghussian, *Thermochim. Acta* **488**, 60 (2009).
21. P. Alizadeh and V. K. Marghussian, *J. Eur. Ceram. Soc.* **20**, 775 (2000).
22. A. Karamanov, P. Pisciella, and M. Pelino, *J. Eur. Ceram. Soc.* **19**, 2641 (1999).
23. Y. J. Park and J. Heo, *J. Hazard. Mater.* **91**, 83 (2002).
24. G. Qian, Y. Song, C. Zhang, Y. Xia, H. Zhang, and P. Chui, *Waste Manage.* **26**, 1462 (2006).
25. L. BarbieRi, C. Leonelli, T. Manfredini, G. C. Pellacani, C. Siligardi, R. Bertoncello, *et al. J. Mater. Sci.* **29**, 6273 (1994).
26. G. A. Khater, *Ceram. Int.* **37**, 2193 (2011).
27. M. Rezvani, B. Efekhari-Tekta, M. Solati-Hashjin, and V. K. Marghussian, *Ceram. Int.* **31**, 75 (2005).
28. A. Karamanov, L. Arrizza, I. Matekovits, and M. Pelino, *Ceram. Int.* **30**, 2129 (2004).
29. S. Suresh, T. Narendrudu, S. Yusub, A. Suneel Kurmar, V. Ravi Kurmar, D. Krishna Rao, *et al. Sepctrochim. Acta A* **153**, 281 (2016).
30. G. A. Khater, M. O. Abu Safiah, and E. M. A. Hamzawy, *Process. Appl. Ceram.* **9**, 117 (2015).
31. A. A. Francis, *Mater. Res. Bull.* **41**, 1146 (2006).
32. H. R. Fernandes, D. U. Tulyaganov, and J. M. F. Ferreira, *J. Mater. Sci.* **48**, 765 (2013).
33. M. M. Kržmanc, U. Došler, and D. Suvorov, *J. Am. Ceram. Soc.* **95**, 1920 (2012).
34. F. Li and X. Liu, *MATEC web of Conferences* 34, 01008 (2015).
35. P. Alizadeh and V. K. Marghussian, *J. Eur. Ceram. Soc.* **20**, 765 (2000).
36. Y. J. Park and J. Hoe, *Ceram. Int.* **28**, 689 (2002).
37. M. L. Ovecoglu, B. Kuban, and H. Ozer, *J. Eur. Ceram. Soc.* **17**, 957 (1997).
38. M. Romero, R. D. Rawlings, and J. Ma. Rincón, *J. Eur. Ceram. Soc.* **19**, 2049 (1999).